JOURNAL OF VIROLOGY, Apr. 1992, p. 1841–1848
0022-538X/92/041841-08$02.00/0

Vol. 66, No. 4

Repair and Mutagenesis of the Genome of a Deletion Mutant of the Coronavirus Mouse Hepatitis Virus by Targeted RNA Recombination

CHERI A. KOETZNER,[1] MONICA M. PARKER,[1] CYNTHIA S. RICARD,[1] LAWRENCE S. STURMAN,[1,2] AND PAUL S. MASTERS[1,2]*

Wadsworth Center for Laboratories and Research, New York State Department of Health, Albany, New York 12201-0509,[1] and Department of Biomedical Sciences, School of Public Health, State University of New York at Albany, Albany, New York 12237[2]

Received 8 November 1991/Accepted 16 December 1991

The genetic characterization of a nucleocapsid (N) protein mutant of the coronavirus mouse hepatitis virus (MHV) is described. The mutant, Albany 4 (Alb4), is both temperature sensitive and thermolabile. Analysis of the progeny of a mixed infection showed that the defective Alb4 allele is recessive to wild type, and its gene product is diffusible. The N protein of Alb4 was found to be smaller than its wild-type counterpart, and sequence analysis of the Alb4 N gene revealed that it contains an internal deletion of 87 nucleotides, producing an in-frame deletion of 29 amino acids. All of these properties of Alb4 made it ideal for use as a recipient in a targeted RNA recombination experiment in which the deletion in Alb4 was repaired by recombination with synthetic RNA7, the smallest MHV subgenomic mRNA. Progeny from a cotransfection of Alb4 genomic RNA and synthetic RNA7 were selected for thermal stability. Polymerase chain reaction analysis of candidate recombinants showed that they had regained the material that is deleted in the Alb4 mutant. They also had acquired a five-nucleotide insertion in the 3′ untranslated region, which had been incorporated into the synthetic RNA7 as a molecular tag. The presence of the tag was directly verified, as well, by sequencing the genomic RNA of purified recombinant viruses. This provided a clear genetic proof that the Alb4 phenotype was due to the observed deletion in the N gene. In addition, these results demonstrated that it is possible to obtain stable, independently replicating progeny from recombination between coronavirus genomic RNA and a tailored, synthetic RNA species.

Coronaviruses are enveloped, positive-strand RNA viruses that are important respiratory, neurologic, and enteric pathogens for humans and domestic animals (14, 29, 31). Their virions, which are roughly spherical, contain two species of transmembrane glycoprotein, the spike glycoprotein (S) and the membrane glycoprotein (M). In some coronaviruses, a third membrane glycoprotein, a hemagglutinin-esterase (HE), is also found. Contained within the virion, and possibly associated with the internal portion of M (32), is a helically symmetric nucleocapsid composed of the RNA genome and multiple monomers of the nucleocapsid protein (N).

Despite having relatively few structural proteins, coronaviruses have the largest genomes among the RNA viruses—some 31,000 nucleotides in the case of mouse hepatitis virus (MHV) (16, 23). Much of this coding capacity may be devoted to the strikingly intricate mechanism of replication and transcription that coronaviruses employ (14, 29, 31). Leader-primed transcription of a full-length negative-strand copy of the genome produces a 3′-coterminal nested set of transcripts. Each subgenomic mRNA thus contains a leader identical to the 5′ extreme of the genome linked to a given gene and all material 3′ to that gene. In addition, each of the subgenomic mRNAs can be amplified independently, via the intermediate synthesis of a negative-strand species of the same size (27, 28). This scheme derives further complexity from the high rate of recombination that occurs during coronavirus replication and which is thought to result from a process of polymerase pausing, detachment, and homologous reattachment during RNA synthesis (2, 4, 9, 10, 12, 17).

As part of an effort to gain insight into the functions and interactions of coronavirus structural proteins, we have previously isolated a set of mutants of MHV (30, 33). In this report, we describe the genetic characterization of one of these, an N gene deletion mutant designated Albany 4 (Alb4). To definitively map the mutation in Alb4, we made use of its unique properties to carry out targeted recombination between synthetic RNA and the MHV genome.

MATERIALS AND METHODS

Virus and cells. MHV-A59 wild-type, mutant, and recombinant virus stocks were grown in mouse 17 clone 1 cells; plaque titrations and plaque purifications were performed in mouse L2 cells. Thermal inactivation experiments were carried out by incubation of released virus in 50 mM Tris-maleate (pH 6.5)–100 mM NaCl–1 mM EDTA–10% fetal bovine serum at 40°C for the periods of time indicated.

Cloning and sequencing of cDNA and construction of transcription vectors. cDNA clones of the N gene of the Alb4 mutant were generated from poly(A)-containing infected cell RNA by a modification of the procedure of Gubler and Hoffman (8) as described previously (24). The sequence of the Alb4 N gene was determined at least once in both directions from a nearly full-length clone, pCR18, which contained the entire coding region and most of the 5′ leader and 3′ untranslated region (UTR). The sequence of the region of the Alb4 deletion was then confirmed on four independent cDNA clones. DNA sequencing was carried out

* Corresponding author.

by the method of Sanger et al. (26), using modified T7 DNA polymerase (Sequenase; U.S. Biochemical) and primers described previously (24).

A bacteriophage T7 RNA polymerase transcription vector expressing the smallest subgenomic RNA (RNA7) of wild-type MHV-A59 was constructed largely from pA15, a cDNA clone of the N gene (24) that contains the entire coding region and most of the 5′ leader and 3′ UTR. Using synthetic oligodeoxynucleotides, the remainder of the MHV-A59 5′ leader and an adjoining T7 promoter were constructed upstream of this region by means of a series of intermediate constructs. The rebuilt gene and promoter were inserted between the *Bam*HI and *Hin*dIII sites of the vector pUC8 (34). Recombinant DNA manipulations were done by standard techniques (18), and all newly generated segments and junctions in the resulting plasmid, pMP304, were verified by DNA sequencing. The T7 promoter used, 5′-TAATACGAC TCACTATAG(+1)G-3′, was chosen to optimize transcription efficiency while incorporating a minimum of heterologous nucleotides into the templated RNA (20). Thus, transcripts from pMP304 and its derivatives had two G residues preceding the authentic MHV-A59 leader, as determined by Lai et al. (15) and Pachuk et al. (23).

The remainder of the 3′ UTR of the N gene was reconstructed by means of reverse transcription of wild-type viral genomic RNA, followed by polymerase chain reaction (PCR). The first-strand primer for this procedure was 5′-CCAAGCTTATGCA$(T)_{14}$-3′, which was designed to prime within the poly(A) tail and also contained *Nsi*I and *Hin*dIII sites at its terminus. The second-strand primer was an oligodeoxynucleotide corresponding to nucleotides 1307 to 1323 of the N gene (24), 88 nucleotides upstream from a *Bst*EII site in the 3′ UTR. The PCR product was restricted with *Bst*EII and *Hin*dIII, and larger fragments [having higher poly(A) content] were gel purified and ligated in place of the *Bst*EII-*Hin*dIII fragment of pMP304. All newly generated segments and junctions in the resulting construct, pCK70, were verified by DNA sequencing; the plasmid was found to contain a poly(A) tract of 100 to 110 residues. Runoff transcription of *Nsi*I-cut pCK70 yielded RNAs terminating in poly(A) with no heterologous nucleotides at the 3′ end.

A derivative of pCK70, containing a five-nucleotide insertion abolishing the *Bst*EII site in the 3′ UTR of the N gene, was created by restriction with *Bst*EII followed by fill-in with Klenow fragment and religation. The resulting plasmid was designated pCK116.

Genome RNA purification, synthesis of subgenomic RNA, and RNA sequencing. For the preparation of viral genomic RNA, virus was purified by polyethylene glycol precipitation, as described previously (32), followed by two cycles of equilibrium centrifugation on potassium tartrate-glycerol gradients (22) containing 50 mM Tris-maleate (pH 6.5)–1 mM EDTA. Purified virus, pelleted by ultracentrifugation, was disrupted with 10 mM Tris-HCl (pH 7.5)–140 mM NaCl–1 mM $MgCl_2$–5 mM EDTA–0.44% Nonidet P-40–1% sodium dodecyl sulfate (SDS) and then extracted twice with phenol-chloroform and twice with chloroform. Following two ethanol precipitations, viral RNA was resuspended in water, aliquoted, and stored on liquid nitrogen.

Subgenomic RNAs were synthesized as capped, runoff transcripts from *Nsi*I-truncated pCK70 and pCK116 essentially as described by Melton et al. (19). Cap analog m^7GpppG and T7 RNA polymerase were obtained from New England Biolabs; RNasin was from Promega. Products were extracted twice with phenol-chloroform and twice with chloroform and were twice precipitated from ethanol. The incorporation of [5,6-^{3}H]UTP (Amersham) was determined by binding of product RNA to DEAE filter paper (Whatman DE81). The size and homogeneity of synthesized RNA were verified by electrophoresis in 5% polyacrylamide gels containing 8 M urea, followed by fluorography.

Sequencing of purified viral genomic RNA was carried out by dideoxy-chain termination (26) using avian myeloblastosis virus reverse transcriptase (Life Sciences). The sequencing primer, complementary to nucleotides 1451 to 1468 of the N gene, was end labeled with [γ-^{32}P]ATP (Amersham) and polynucleotide kinase (New England Biolabs).

Transfection and recombinant selection. Alb4 genomic and synthetic subgenomic RNAs were cotransfected into 17 clone 1 cells, using 800 μg of DEAE-dextran (Pharmacia) per ml in IRA buffer (21). In our hands, higher RNA transfection efficiencies were obtained with trypsinized cells transfected in suspension (7) for 2 h at 33°C. Cells were then seeded into T25 flasks and incubated at 33°C until the appearance of extensive syncytia and cytopathic effect on the monolayers (24 to 29 h). A portion of the released virus was thermally inactivated for 24 h at 40°C, and survivors forming large plaques at 39°C were obtained by plaque titration on L2 cells. These candidate recombinants were plaque purified once and subsequently passaged in 17 clone 1 cells.

PCR. Purified viral genomic RNA from candidate recombinants, the wild type, and Alb4 was reverse transcribed by using a primer complementary to nucleotides 1632 to 1649 of the N gene. This and a second primer, corresponding to nucleotides 1077 to 1094, were then used in 100 μl of DNA amplification reaction mixtures containing 67 mM Tris-HCl (pH 8.8) (at ambient temperature), 16.7 mM $(NH_4)_2SO_4$, 3.0 mM $MgCl_2$, 10 mM β-mercaptoethanol, 170 μg of bovine serum albumin per ml, 290 μM deoxynucleotide triphosphates (dNTPs), 60 pmol of each primer, and 2.5 U of *Taq* polymerase (Perkin-Elmer Cetus). Reactions were run for 30 cycles of 1 min at 94°C, 1 min at 45°C, and 4 min at 72°C in a DNA thermal cycler (Perkin-Elmer Cetus). PCR products were extracted twice with phenol-chloroform and twice with chloroform and were twice ethanol precipitated from 2 M ammonium acetate to remove precursor dNTPs (8). PCR products were analyzed by electrophoresis on 1.5% agarose.

Nucleotide sequence accession number. The sequence reported here has been assigned GenBank accession number M80644.

RESULTS

Identification of an N gene mutant of MHV. The Alb4 mutant was obtained as a member of a set of temperature-sensitive mutants of MHV-A59 selected for alterations in production of cytopathic effect at the nonpermissive temperature, 39°C (30, 33). Two important aspects of the phenotype of Alb4 were found. First, the mutant is temperature sensitive, forming very small plaques on either 17 clone 1 cells or L2 cells at the nonpermissive temperature. After 48 h at 39°C, Alb4 plaques are 1.0 to 1.5 mm in diameter, compared with 3.5 to 4.0 mm for wild-type virus. By contrast, no plaque size difference is detectable at the permissive temperature, 33°C. The second critical aspect of the phenotype of Alb4 is that it is markedly thermolabile. Incubation of mutant virus at 40°C, pH 6.5, results in a relatively rapid loss of infectious titer. A typical course of thermal inactivation is shown in Fig. 1A. In this experiment, heat treatment of Alb4 for 4 h produced a greater than 10-fold decrease in PFU (titered at the permissive temperature), while under the same conditions wild-type virus was practically unaffected. By 24

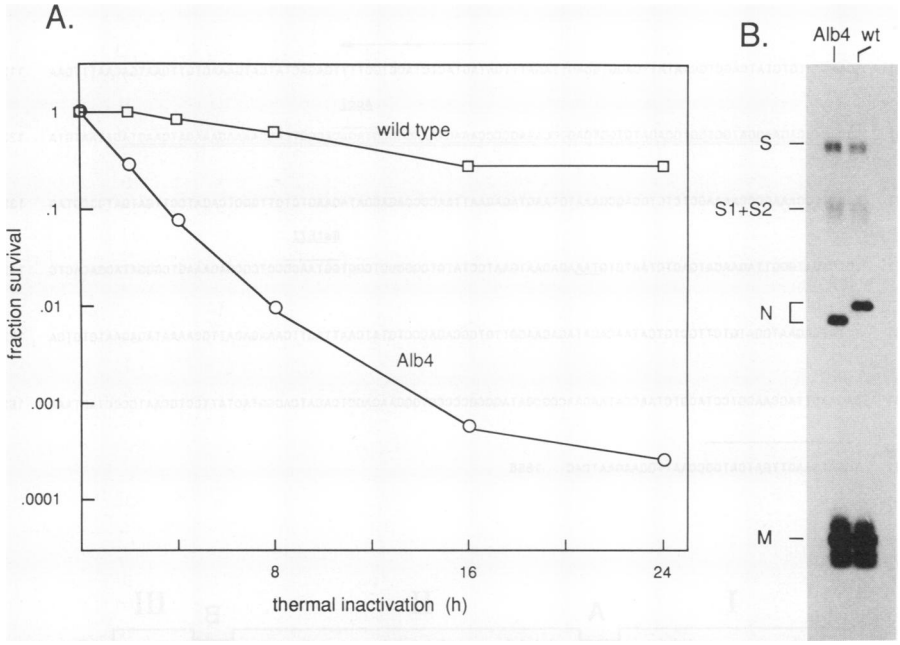

FIG. 1. Characteristics of Alb4 virions. (A) Thermal inactivation of virions. Wild-type virus (4.4×10^8 PFU/ml) and Alb4 virus (4.3×10^8 PFU/ml) were diluted 250-fold and thermally inactivated as described in Materials and Methods. Surviving viruses were titered at 33°C. (B) Structural protein composition of Alb4 and wild-type (wt) virions. Viruses were radiolabeled with [^{35}S]methionine and purified on sucrose density gradients as described previously (32). Equal amounts of each virus, as estimated by both counts per minute and protein determination, were analyzed by SDS-PAGE (13) and fluorography.

h of heat treatment, the infectious titer of Alb4 had dropped 4,000-fold, whereas that of the wild type underwent less than a 4-fold reduction. This direct thermolability of Alb4 virions strongly suggested that the defect in the mutant must reside in a gene encoding one of the three viral structural proteins or, conceivably, in some structural element of the RNA genome that could be irreversibly altered by heat treatment.

Recessive character of the Alb4 mutation. To gain more information about the lesion in Alb4, the progeny of a mixed infection by wild-type and Alb4 viruses were examined. Both viruses, either individually or in combination, were used to infect cells at the permissive temperature. The multiplicity of infection, 5 PFU per cell for each virus, was such that in the mixed infection we expected >98% of cells to be doubly infected by mutant and wild-type viruses. The resulting progeny were either left untreated or subjected to a 24-h heat treatment. The composition and thermolability of progeny were then determined by plaque titration at both 33 and 39°C.

As shown in the final two columns of Table 1, a mixed infection by wild-type and Alb4 virus produced roughly equal numbers of progeny of each, as judged by the numbers of large and small plaques obtained from titration at 39°C prior to heat treatment. Following heat treatment of the mixed-infection progeny virus, the titers of large plaques and small plaques dropped 2.8- and 8.2-fold, respectively. This latter value differed markedly from the 250-fold drop in titer that was observed following heat treatment of Alb4 virus alone, and it more closely resembled the 3.9-fold drop in titer brought about by heat treatment of wild-type virus alone. Thus, Alb4 virions resulting from a mixed infection with wild-type virus were initially protected from the effects of heat treatment (to a similar extent as with the wild type). This protection was not heritable, however, and Alb4 virus subsequently produced small plaques at the nonpermissive temperature. These results suggested that the mutant allele in Alb4 is recessive to its wild-type counterpart and that its gene product is diffusible. Mixing of mutant and wild-type gene products during assembly of progeny virions allowed for a protection of progeny against the effects of thermal inactivation, but this protection was lost when individual virions were then propagated in a plaque assay. These results also appear to rule out the possibility that an altered genomic RNA structural element is responsible for the Alb4 phenotype.

Alb4 virion proteins. Further support for the notion of a structural gene lesion in Alb4 came from examination of virion proteins of the mutant (30, 33). Cells infected with Alb4 or wild-type virus at 33°C were labeled with [^{35}S]methionine, and purified virions were analyzed by SDS-polyacrylamide gel electrophoresis (PAGE). As shown in Fig.

TABLE 1. Thermolability of progeny of a mixed infection of wild-type and Alb4 viruses[a]

Virus	Thermal inactivation	Total titer		Large plaques, 39°C	Small plaques, 39°C
		33°C	39°C		
Wild type		5.8×10^6	5.5×10^6	5.5×10^6	0
	24 h	1.6×10^6	1.4×10^6	1.4×10^6	0
Alb4		1.2×10^6	7.7×10^5	0	7.7×10^5
	24 h	ND[b]	3.1×10^3	0	3.1×10^3
Wild type and Alb4		1.7×10^6	1.2×10^6	5.9×10^5	6.0×10^5
	24 h	2.4×10^5	2.8×10^5	2.1×10^5	7.3×10^4

[a] Wild-type virus (at 5 PFU per cell), Alb4 virus (at 5 PFU per cell), or both (each at 5 PFU per cell) were used to infect 17 clone 1 cells at 33°C. Released virus, harvested 18 h postinfection, was diluted 10-fold into buffer (Materials and Methods) and was held untreated or was thermally inactivated at 39°C for 24 h.

[b] ND, not determined.

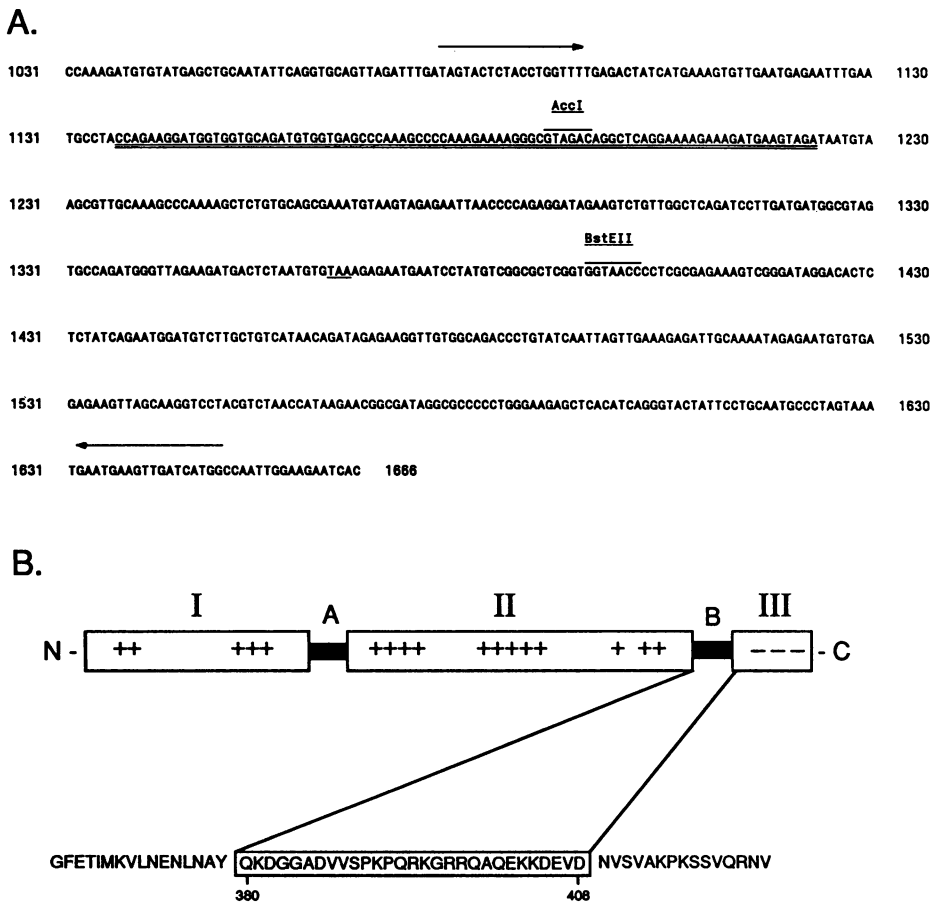

FIG. 2. Alb4 N gene and protein sequence. (A) The distal portion of the wild-type MHV-A59 N gene sequence, including the entire 3′ UTR, exclusive of polyadenylate. Nucleotide residues deleted in Alb4 are doubly underlined. Numbering begins with the first base of the N gene start codon, as given previously (24). The N gene stop codon is singly underlined. The positions of the PCR primers (denoted by arrows) and the *Acc*I and *Bst*EII sites used in PCR analysis are indicated. Residue 1613, previously reported as a T (24), has been found to be a C in our strain of MHV-A59. (B) A portion of the MHV-A59 N protein sequence, showing the residues deleted in the Alb4 N protein (boxed). The sequence is given in the context of a three-domain model of the MHV N protein described previously (24).

1B, the N protein of Alb4 had a greater mobility than did wild-type N protein, although its stoichiometry relative to the other viral proteins was not significantly altered. No quantitative or qualitative differences were noted between the S or M proteins of mutant and wild-type virions. Since virus was grown at the permissive temperature, this finding strongly suggested that the N gene of Alb4 contains a substantial deletion. Alternatively, it may have indicated a differential extent of posttranslational modification or greater protease susceptibility of Alb4 N compared with wild-type N.

Sequence of the Alb4 N gene. The salient difference between the N proteins of wild type and Alb4 made it of interest to compare their gene sequences. The N gene sequence of Alb4 was determined from cloned cDNAs and was found to contain a deletion of 87 nucleotides in the distal portion of the coding region (Fig. 2A). The remainder of the Alb4 N gene coding region was everywhere else identical to that of its wild-type MHV-A59 parent (24; GenBank accession number M35256). Moreover, there were no changes in the 62 nucleotides of the 5′ leader or the 274 nucleotides of the 3′ UTR contained in the largest Alb4 cDNA clone. The Alb4 deletion results in an in-frame deletion of 29 amino acids, residues 380 through 408, of the 454 amino acid N protein (Fig. 2B). There is no change in the amino acid encoded at the boundaries of the deletion, although the tyrosine codon situated at this junction is altered from TAC to TAT (Fig. 2A).

Targeted recombination between synthetic RNA and the Alb4 genome. The large deletion in the Alb4 N gene appeared likely to be the mutation conferring the properties of temperature sensitivity and thermolability on this mutant. However, as yet there was no strong genetic evidence for such a conclusion. It thus became of interest to try to repair the deletion in the Alb4 genome, using in vitro-synthesized RNA containing the missing wild-type sequence. The reasons for attempting this were twofold. First, it would genetically prove or disprove whether the deletion in Alb4 was indeed responsible for the observed phenotype of that mutant. Second, it would provide a potential means for site-directed mutagenesis of the genome of MHV, at least in the neighborhood of the N gene.

MHV undergoes a high rate of RNA recombination (2, 4, 9, 10, 12, 17), and this is presumed to occur via a template switching mechanism (4, 17). In addition, it has recently been shown that subgenomic replicons contribute to the amplification of coronavirus mRNA during infection (27, 28). Both genomic and subgenomic RNAs have the same 5′ and

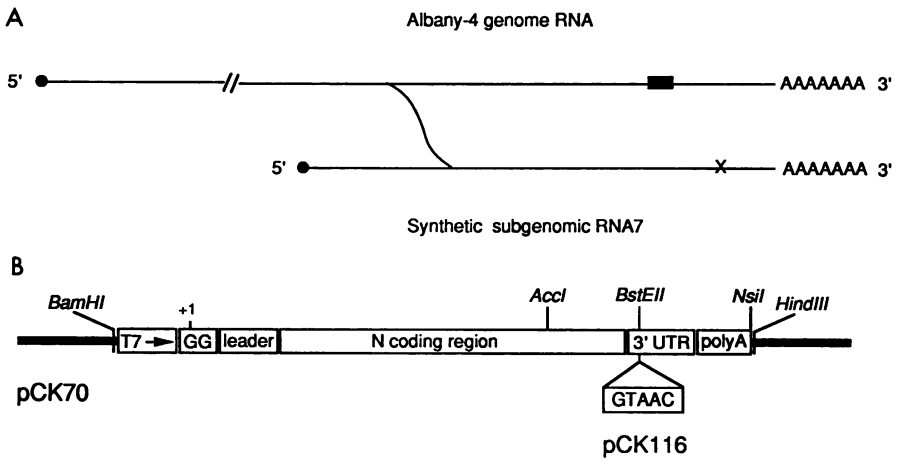

FIG. 3. Strategy for targeted RNA recombination. (A) Schematic of a possible single crossover between Alb4 genomic RNA and synthetic subgenomic RNA7. The solid rectangle represents the deletion in Alb4. A mutation, which could potentially be cotransduced into the genomic RNA along with the RNA repairing the deletion, is indicated by ×. In principle, the mutation could be either 5′ or 3′ to the deletion locus. Note that the hypothetical recombination event might occur during either positive- or negative-strand synthesis. (B) Transcription vectors used for synthesis of MHV subgenomic RNA7. The construction of pCK70 and pCK116 is described in Materials and Methods. Vector pCK70, when linearized with *Nsi*I, serves as a template for transcription of the authentic polyadenylated MHV-A59 RNA7 sequence with two additional G residues at the 5′ end and no heterologous bases at the 3′ end. Vector pCK116 is identical to pCK70 except for a five-nucleotide insertion that abolishes the *Bst*EII site in the 3′ UTR.

3′ termini and are probably recognized similarly by the viral polymerase as templates during negative- and positive-strand RNA synthesis. It appeared likely, then, that recombination events between subgenomic and genomic RNAs might contribute substantially to the overall observed rate of recombination.

Our strategy for repairing the deletion in Alb4 was to transfect cells with Alb4 genome RNA and wild-type subgenomic RNA7, the smallest MHV subgenomic RNA, which is a monocistronic mRNA for the N gene. It was expected that the simplest event capable of repairing the Alb4 deletion would be a single crossover that might occur during either negative- or positive-strand RNA synthesis, as shown schematically in Fig. 3A. If repair of the deletion generated heat-stable recombinants, these could then be selected as survivors of a thermal inactivation step. Revertants of Alb4, which are due to second-site point mutations, arise at a frequency of roughly 10^{-6} per passage (11). Thus, if the frequency of the targeted recombination were of this order or higher, then we expected to be able to detect recombinants.

Wild-type MHV-A59 subgenomic RNA7 was synthesized from a vector, pCK70 (Fig. 3B), which was designed to template synthesis of an RNA species differing from authentic RNA7 only by the presence of two additional G residues at its 5′ terminus. The positive- and negative-strand template requirements of the MHV RNA polymerase have not yet been defined, so it is unclear whether this degree of stringency was necessary. Synthetic RNA7 and purified Alb4 genome RNA were cotransfected into cells by using DEAE-dextran. It was thought that this would increase the chances of the anticipated recombination event by ensuring that successfully transfected cells would contain both RNA species. Released virus from the cotransfection was harvested and thermally inactivated, and survivors were selected by plaque titration at the nonpermissive temperature. In the initial experiment, two of six independent cotransfections yielded numerous large-plaque survivors which, by PCR analysis, were determined to have regained the material deleted in the Alb4 mutant (data not shown). However, since these putative recombinants were indistinguishable from wild-type virus, it could be argued that they were, in fact, contaminating wild-type virus from an exogenous source.

To test whether recombination had actually occurred, a molecular tag was incorporated into the synthetic RNA7. This was done by creating a five-nucleotide insertion at a unique *Bst*EII site in the proximal portion of the 3′ UTR, 30 nucleotides beyond the N gene stop codon (Fig. 2A). In the resulting vector, pCK116 (Fig. 3B), this insertion disrupted the *Bst*EII site. Unless this mutation were deleterious to the virus, it appeared likely that most recombination events between synthetic RNA and Alb4 genomic RNA would cotransduce the five-nucleotide insertion along with the material repairing the deletion. Recombinants would thus contain a specific mutation not found in wild-type MHV.

The cotransfection experiment was repeated, using synthetic RNA7 (derived from pCK116) and Alb4 genomic RNA at molar ratios of 10:1 and 100:1. Large-plaque survivors were obtained in two of eight independent cotransfections, and four of these candidate recombinants, designated Alb46 to Alb49, were purified and passaged for further analysis. Purified viral genomic RNA from the wild type, Alb4, and Alb46 to Alb49 was reverse transcribed and amplified by PCR, using a pair of primers spanning the region containing both the deletion and the five-nucleotide insertion (Fig. 2A). For the recombinants, this was predicted to produce a DNA fragment of 578 bp, compared with 573 bp for wild-type virus and 486 bp for Alb4. As shown in Fig. 4, PCR products from the recombinants were the same size as that from the wild type and clearly larger than that from Alb4, consistent with repair of the deletion in these viruses.

The DNA copy of the portion of the N gene that is missing in Alb4 contains a unique *Acc*I site (Fig. 2A), which should have been restored in the recombinants. Figure 4A demonstrates that PCR products from wild-type and recombinant viruses were sensitive to cutting by *Acc*I, and all produced restriction fragments consistent with the predicted sizes of

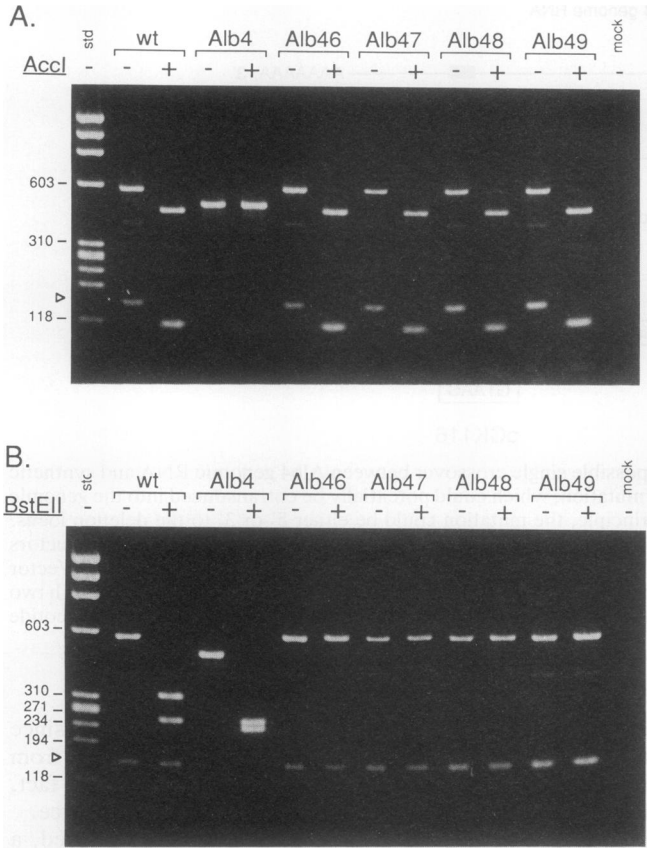

FIG. 4. PCR analysis of recombinants. Reverse transcription followed by PCR was used to amplify a portion of purified genome RNA from wild-type (wt), Alb4, and recombinant viruses Alb46 to Alb49 as detailed in Materials and Methods. PCR products, before and after digestion with either *Acc*I (A) or *Bst*EII (B), were analyzed by electrophoresis on 1.5% agarose stained with ethidium bromide. Sizes (in base pairs) of relevant fragments of a *Hae*III-digested ϕX174 replicative-form DNA standard (std; New England Biolabs) are indicated on the left. The open arrowhead indicates a minor band, thought to be a product of mispriming, that appeared in all wild-type and recombinant PCR products but not in those of Alb4. A mock reaction (last lane) containing no viral RNA was processed identically to the other reactions.

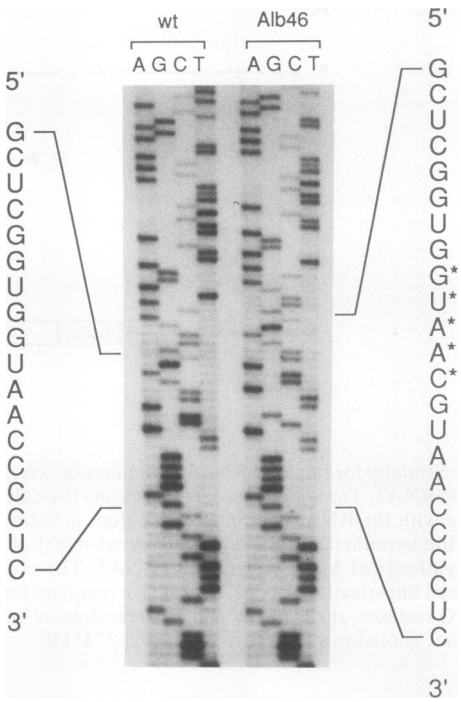

FIG. 5. Genomic RNA sequences of wild-type and recombinant Alb46 viruses. Wild-type (wt) and Alb46 (passage level 4) virions were purified through two cycles of equilibrium centrifugation on tartrate-glycerol gradients, and RNA purified from these was sequenced by dideoxy-chain termination. The autoradiogram shows a region in the proximal portion of the 3′ UTR. The indicated segment of sequence is given as positive-sense RNA. Asterisks highlight the five-nucleotide insertion in Alb46.

116 and 457 bp (or 462 bp). As expected, the PCR product from Alb4 could not be cut by *Acc*I.

The construction of the five-nucleotide insertion abolished the *Bst*EII site in the DNA copy of the 3′ UTR (Fig. 2A and 3B). Thus, this site should have been absent from the recombinants but undisturbed in wild-type and Alb4 viruses. Figure 4B shows that PCR products from Alb46 to Alb49 could not be cut by *Bst*EII. This did not indicate a general refractoriness toward restriction digestion, since these same PCR products had been sensitive to *Acc*I. As expected, PCR products from the wild type and Alb4 could be cut by *Bst*EII, and the two produced one set of identically sized fragments and one set differing by the size of the deletion. Taken together, these results demonstrated that the recombinants were indistinguishable from wild-type virus in the region of the deletion but that they differed from the wild type in the proximal portion of the 3′ UTR as the result of an engineered mutation.

To confirm the nature of the *Bst*EII resistance in the recombinants, we directly sequenced purified viral genomic RNA from Alb46 and wild-type virus. As shown in Fig. 5, the identical five-nucleotide insert that had been created in the transcription vector pCK116 was present in the genome of Alb46. The presence of the same insert in Alb47 and its absence in Alb4 were also verified by sequencing genomic RNA (data not shown).

The phenotype of the recombinants provided clear genetic proof that the deletion found in Alb4 is the mutation responsible for the phenotype of this mutant. Restoration of the deleted material generated viruses that survived thermal inactivation and formed large (wild-type-sized) plaques at the nonpermissive temperature. The results also demonstrated that it is possible to obtain stable, independently replicating progeny from recombination between coronavirus genomic RNA and a tailored, synthetic RNA species.

DISCUSSION

The genetic characterization of the Alb4 mutant in this report provides new information about the N protein of MHV as well as a potential tool for future studies. On the basis of a sequence comparison of the N genes of five strains of MHV, we have previously suggested as a working model that the N protein consists of three structural domains separated by two spacer regions (24). It was proposed that, in contrast to the highly conserved domains I, II, and III, the compositions of the more variable spacers A and B were relatively unimportant and that these regions primarily serve as connectors (Fig. 2B). The sequence of the Alb4 mutant

shows this notion to be at least partially correct. The deletion in Alb4 almost exactly coincides with spacer B. Therefore, this region is largely dispensable for N protein function, since Alb4 is completely viable at the permissive temperature and is even partially viable at the nonpermissive temperature. With respect to this conclusion, it should be noted that the deletion in Alb4 falls entirely outside of a second, internal open reading frame found within the N gene (24), and thus the N protein is most likely the only gene product affected.

It is unclear at this point what the thermolability of the Alb4 N protein means. Heat treatment of Alb4 virions results in their killing, or at least in their inability to be propagated for sufficient generations to form detectable plaques. Possibly, heat treatment leads to a lethal uncoating defect such that incoming viral genomes cannot be translated. Alternatively, the heat-altered Alb4 N protein may fail to sufficiently protect the genome against cellular RNases encountered on the pathway to internalization of infecting virions. We are currently seeking biochemical evidence to complement our present genetic picture of the Alb4 lesion.

Our study has taken advantage of the high rate of homologous RNA recombination that occurs during coronavirus replication. A large body of work has demonstrated that coronavirus recombination occurs among selected and unselected markers in tissue culture (2, 4, 10, 17), in inoculated laboratory animals (9), and in the wild (12). For MHV, recombination takes place across the entire length of the genome (10) at a sufficiently uniform rate to allow construction of a classical genetic map (4). A recent study suggests that on a fine scale, recombination is virtually random (3), although selective pressures may create the appearance of local clustering of recombinational hot spots (2).

Recombination in MHV is thought to take place as a result of switching by the viral RNA polymerase between homologous positions on different templates (4, 17). Since coronavirus subgenomic RNAs are also independently amplified by the viral polymerase (27, 28), we reasoned that these active templates for RNA synthesis might participate in a substantial fraction of recombination events. It should be noted, however, that our ability to obtain targeted recombinants does not necessarily imply the mechanism by which they arose. The work presented here does not show that the cotransfected RNA7 species were amplified, as occurs in situ (27, 28). Moreover, we have not addressed the issues of whether the targeted recombination occurred by a simple single crossover, as hypothesized in Fig. 3A, or whether recombination took place during negative- or positive-strand synthesis.

Irrespective of mechanism, however, it is clear that the expected recombinants were obtained, and it is hoped that this method will be generally useful in constructing other targeted mutations. The five-nucleotide insertion at the *Bst*EII site within the 3′ UTR was constructed to provide a selectively neutral molecular tag to label recombinants. Two other coronaviruses, transmissible gastroenteritis virus and feline infectious peritonitis virus, have one or more additional genes at an analogous position distal to the N gene (29). Thus, we speculated that this might be a locus tolerant to some degree of sequence change. This appears to have been a correct assumption, since the recombinants obtained are phenotypically similar, if not identical, to wild-type virus.

Site-specific mutagenesis of an RNA virus was first achieved with poliovirus, as a result of the production of a full-length infectious cDNA (25). Similar full-length constructs have revolutionized the genetic analysis of a number of other positive-strand viruses. The construction of an analogous full-length coronavirus clone, however, will likely be a prodigious technical feat owing to the huge size of coronavirus genomes (ca. 26 to 31 kb). The ability to obtain recombination between genomic and engineered RNA molecules has been demonstrated previously for brome mosaic virus (5), cowpea chlorotic mottle virus (1), turnip crinkle virus (6), and Sindbis virus (35). For coronaviruses, targeted RNA recombination might be a useful alternative for the generation of both specific and random mutations for studies of gene expression and function.

The construction of the recombinants reported here was dependent on the powerful counterselection provided by the thermolability of the Alb4 mutant. From the data currently available, we would roughly estimate the frequency of recovery of targeted recombinants by our protocol to be on the order of 10^{-5}. Although this is sufficiently higher than the reversion frequency of Alb4, it may be too low to allow direct identification of recombinants (e.g., by plaque hybridization) without counterselection against the parental virus. Thus, our present scheme for targeted recombination is limited to the neighborhood of the 3′ end of the MHV genome, and it also could not be used to introduce mutations which, by themselves, would be deleterious to viral viability. In principle, other coronavirus temperature-sensitive mutants with low reversion frequencies could be used as recipients in similar selection schemes to mutagenize different regions of the genome. A more general applicability of targeted RNA recombination, however, may require finding conditions that favor higher rates of recombination of exogenous RNA. In this regard, the use of negative-strand subgenomic RNA (excluding antileader) should be considered, since it is possible that the viral polymerase may accept this as a substrate to be extended to yield full-length antigenome. In addition, the frequency of targeted recombination may be enhanced if the subgenomic RNA species is transfected into cells which have already been infected for various periods of time. A recent study has presented evidence that the rate of MHV recombination is increased at later times postinfection (4). We are presently seeking to further optimize the frequencies of RNA transfection and recombination in our system and to construct new mutants.

ACKNOWLEDGMENTS

We are grateful to Dorothea Sawicki, Arlene Ramsingh, Dorothy Young, and David Anders for advice on transfections. We thank Jill Taylor and Ding Peng for critically reading the manuscript.

This work was supported in part by Public Health Service grants GM31698 (L.S.S.) and AI31622 (P.S.M.) from the National Institutes of Health.

REFERENCES

1. **Allison, R., C. Thompson, and P. Ahlquist.** 1990. Regeneration of a functional RNA virus genome by recombination between deletion mutants and requirement for cowpea chlorotic mottle virus 3a and coat genes for systemic infection. Proc. Natl. Acad. Sci. USA **87**:1820–1824.
2. **Banner, L. R., J. G. Keck, and M. M. C. Lai.** 1990. A clustering of RNA recombination sites adjacent to a hypervariable region of the peplomer gene of murine coronavirus. Virology **175**:548–555.
3. **Banner, L. R., and M. M. C. Lai.** 1991. Random nature of coronavirus RNA recombination in the absence of selective pressure. Virology **185**:441–445.
4. **Baric, R. S., K. Fu, M. C. Schaad, and S. A. Stohlman.** 1990. Establishing a genetic recombination map for murine coronavi-

rus strain A59 complementation groups. Virology **177**:646–656.
5. **Bujarski, J. J., and P. Kaesberg.** 1986. Genetic recombination between RNA components of a multipartite plant virus. Nature (London) **321**:528–531.
6. **Collmer, C. W., L. Stenzler, N. Fay, and S. H. Howell.** 1991. Nonmutant forms of the avirulent satellite D of turnip crinkle virus are produced following inoculation of plants with mutant forms synthesized in vitro. Virology **183**:251–259.
7. **Golub, E. I., H. Kim, and D. J. Volsky.** 1989. Transfection of DNA into adherent cells by DEAE-dextran/DMSO method increases drastically if the cells are removed from surface and treated in suspension. Nucleic Acids Res. **17**:4902.
8. **Gubler, U., and B. J. Hoffman.** 1983. A simple and very efficient method for generating cDNA libraries. Gene **25**:263–269.
9. **Keck, J. G., G. K. Matsushima, S. Makino, J. O. Fleming, D. M. Vannier, S. A. Stohlman, and M. M. C. Lai.** 1988. In vivo RNA-RNA recombination of coronavirus in mouse brain. J. Virol. **62**:1810–1813.
10. **Keck, J. G., L. H. Soe, S. Makino, S. A. Stohlman, and M. M. C. Lai.** 1988. RNA recombination of murine coronaviruses: recombination between fusion-positive mouse hepatitis virus A59 and fusion-negative mouse hepatitis virus 2. J. Virol. **62**:1989–1998.
11. **Koetzner, C. A., D. Peng, and P. S. Masters.** Unpublished data.
12. **Kusters, J. G., E. J. Jager, H. G. M. Niesters, and B. A. M. van der Zeijst.** 1990. Sequence evidence for RNA recombination in field isolates of avian coronavirus infectious bronchitis virus. Vaccine **8**:605–608.
13. **Laemmli, U. K.** 1970. Cleavage of structural proteins during the assembly of the head of bacteriophage T4. Nature (London) **227**:680–685.
14. **Lai, M. M. C.** 1990. Coronavirus: organization, replication and expression of genome. Annu. Rev. Microbiol. **44**:303–333.
15. **Lai, M. M. C., R. S. Baric, P. R. Brayton, and S. A. Stohlman.** 1984. Characterization of leader RNA sequences on the virion and mRNAs of mouse hepatitis virus, a cytoplasmic RNA virus. Proc. Natl. Acad. Sci. USA **81**:3626–3630.
16. **Lee, H.-J., C.-K. Shieh, A. E. Gorbalenya, E. V. Koonin, N. La Monica, J. Tuler, A. Bagdzhadzhyan, and M. M. C. Lai.** 1991. The complete sequence (22 kilobases) of murine coronavirus gene 1 encoding the putative proteases and RNA polymerase. Virology **180**:567–582.
17. **Makino, S., J. G. Keck, S. A. Stohlman, and M. M. C. Lai.** 1986. High frequency RNA recombination of murine coronaviruses. J. Virol. **57**:729–737.
18. **Maniatis, T., E. F. Fritsch, and J. Sambrook.** 1982. Molecular cloning: a laboratory manual. Cold Spring Harbor Laboratory, Cold Spring Harbor, N.Y.
19. **Melton, D. A., P. A. Krieg, M. R. Rebagliati, T. Maniatis, K. Zinn, and M. R. Green.** 1984. Efficient in vitro synthesis of biologically active RNA and RNA hybridization probes from plasmids containing a bacteriophage SP6 promoter. Nucleic Acids Res. **12**:7035–7056.
20. **Milligan, J. F., D. R. Groebe, G. W. Witherell, and O. C. Uhlenbeck.** 1987. Oligoribonucleotide synthesis using T7 RNA polymerase and synthetic DNA templates. Nucleic Acids Res. **15**:8783–8798.
21. **Mizutani, S., and R. J. Colonno.** 1985. In vitro synthesis of an infectious RNA from cDNA clones of human rhinovirus type 14. J. Virol. **56**:628–632.
22. **Obijeski, J. F., A. T. Marchenko, D. H. L. Bishop, B. W. Cann, and F. A. Murphy.** 1974. Comparative electrophoretic analysis of the virus proteins of four rhabdoviruses. J. Gen. Virol. **22**:21–33.
23. **Pachuk, C. J., P. J. Bredenbeek, P. W. Zoltick, W. J. M. Spaan, and Susan R. Weiss.** 1989. Molecular cloning of the gene encoding the putative polymerase of mouse hepatitis coronavirus, strain A59. Virology **171**:141–148.
24. **Parker, M. M., and P. S. Masters.** 1990. Sequence comparison of the N genes of five strains of the coronavirus mouse hepatitis virus suggests a three domain structure for the nucleocapsid protein. Virology **179**:463–468.
25. **Racaniello, V. R., and D. Baltimore.** 1981. Cloned poliovirus cDNA is infectious in mammalian cells. Science **214**:916–919.
26. **Sanger, F., S. Nicklen, and A. R. Coulson.** 1977. DNA sequencing with chain-terminating inhibitors. Proc. Natl. Acad. Sci. USA **74**:5463–5467.
27. **Sawicki, S. G., and D. L. Sawicki.** 1990. Coronavirus transcription: subgenomic mouse hepatitis virus replicative intermediates function in RNA synthesis. J. Virol. **64**:1050–1056.
28. **Sethna, P. B., S.-L. Hung, and D. A. Brian.** 1989. Coronavirus subgenomic minus-strand RNAs and the potential for mRNA replicons. Proc. Natl. Acad. Sci. USA **86**:5626–5630.
29. **Spaan, W., D. Cavanagh, and M. C. Horzinek.** 1988. Coronaviruses: structure and genome expression. J. Gen. Virol. **69**:2939–2952.
30. **Sturman, L. S., C. Eastwood, M. F. Frana, C. Duchala, F. Baker, C. S. Ricard, S. G. Sawicki, and K. V. Holmes.** 1987. Temperature-sensitive mutants of MHV-A59. Adv. Exp. Med. Biol. **218**:159–168.
31. **Sturman, L. S., and K. V. Holmes.** 1983. The molecular biology of coronaviruses. Adv. Virus Res. **28**:35–111.
32. **Sturman, L. S., K. V. Holmes, and J. Behnke.** 1980. Isolation of coronavirus envelope glycoproteins and interaction with the viral nucleocapsid. J. Virol. **33**:449–462.
33. **Sturman, L. S., C. A. Koetzner, M. F. Frana, C. Duchala, C. S. Ricard, S. G. Sawicki, J. L. Gombold, S. R. Weiss, and K. V. Holmes.** Unpublished data.
34. **Vieira, J., and J. Messing.** 1982. The pUC plasmids, an M13mp7-derived system for insertion mutagenesis and sequencing with synthetic universal primers. Gene **19**:259–268.
35. **Weiss, B. G., and S. Schlesinger.** 1991. Recombination between Sindbis virus RNAs. J. Virol. **65**:4017–4025.